Catalysis Today xxx (2016) xxx–xxx

Contents lists available at ScienceDirect

Catalysis Today

journal homepage: www.elsevier.com/locate/cattod

Synthesis of hydrogen peroxide over $Pd/SiO_2/COR$ monolith catalysts by anthraquinone method

Yanyan Guo [a], Chengna Dai [a], Zhigang Lei [a,*], Biaohua Chen [a], Xiangchen Fang [b,*]

[a] State Key Laboratory of Chemical Resource Engineering, Beijing University of Chemical Technology, Box 266, Beijing, 100029, China
[b] Fushun Research Institute of Petroleum and Petrochemicals, SINOPEC, Liaoning Fushun, 113001, China

ARTICLE INFO

Article history:
Received 28 October 2015
Received in revised form 9 March 2016
Accepted 11 March 2016
Available online xxx

Keywords:
Catalytic hydrogenation
H_2O_2
$Pd/SiO_2/COR$
Monolith catalyst
Anthraquinone process

ABSTRACT

In this work, a series of $Pd/SiO_2/COR$ (cordierite) catalysts with different Pd contents were successfully prepared by impregnation method. The obtained $Pd/SiO_2/COR$ catalyst samples were characterized by X-ray diffraction (XRD), scanning electron microscopy (SEM), high-resolution transmission electron microscopy (HRTEM), BET, hydrogen temperature programmed reduction (H_2-TPR), inductively coupled plasma-atomic emission spectrometry (ICP-AES), and X-ray photoelectron spectroscopy (XPS). X-ray photoelectron spectroscopy (XPS) show that Pd element is mainly in the state of PdO, and 1.5% $Pd/SiO_2/COR$ catalyst with the theoretical Pd content of 1.5% has the most PdO content on the monolith channel surface when compared to other Pd content monolith catalysts in this paper. Then in the experiment it was found the optimum catalyst is 1.5% $Pd/SiO_2/COR$, which is consistent with XPS results. The STY can achieve 793.2 g H_2O_2 g^{-1} Pd h^{-1} over 1.5% $Pd/SiO_2/COR$ catalyst.

1. Introduction

Hydrogen peroxide (H_2O_2) is an important green chemical raw material and product widely used as oxidant, bleach, disinfectant, deoxidizer, polymer initiator and crosslinking agent. Its applications include military, textile, papermaking, chemical, pharmaceutical, environmental protection, food industries, and others [1,2].

Previously, hydrogen peroxide was mainly prepared by hydrolysis of the ammonium peroxydisulfate. Today, more than 99% of hydrogen peroxide is commercially manufactured by the anthraquinone method, including the 2-ethyl-9,10-anthraquinone (eAQ) hydrogenation process and the autoxidation process of 2-ethyl-9,10-anthrahydroquinone ($eAQH_2$, one of products of eAQ hydrogenation process), while the catalytic hydrogenation of eAQ process is the key step [3–8]. As the target product of hydrogenation of eAQ process, $eAQH_2$ is formed in the quinone-hydroquinone stage but undergoes further hydrogenation reaction. The by-products mainly include 2-ethyl-5,6,7,8-tetrahydroanthracene-9,10-diol and 2-ethyl-1,2,3,4-tetrahydroanthracene-9,10-diol (H_4eAQH_2), and 2-ethyl-1,2,3,4,5,6,7,8-tetrahydroanthracene-9,10-diol (H_8eAQH_2). H_4eAQH_2 is the only desired compound among all of the by-products, because it produces H_2O_2 in the autoxidation process. Meanwhile, H_8eAQH_2 does not produce H_2O_2, so it can be called non-active product [6,7,9,10–14].

The hydrogenation process requires a catalyst, and currently palladium-based pellet catalysts are mainly used in industrial applications [7,15–25]. Halder and Lawal [22] conducted the reaction in a microreactor with inner diameter 0.775 mm and the loading 13 mg supported Pd catalyst (1% Pd). Drelinkiewicz et al. [26] prepared hydrogen peroxide over palladium-based pellet catalyst in a turbulence reactor with the diameter 5.4 cm and the loading 19 g (25 cm^3) supported Pd catalyst (2% Pd). Edvinsson et al. [27] reported the synthesis of H_2O_2 in a commercial slurry reactor at 55 °C and 200 kPa. In recent years, as a kind of novel catalysts, monolithic honeycomb catalysts are widely used in gas, liquid and multiphase systems due to their unique characteristics such as low pressure drop, high specific external surface area and effectiveness factor, minimum axial dispersion, and less catalyst attrition [28–32].

Structured catalysts may have great potential to improve the conversion or selectivity during the anthraquinone hydrogenation process [33,34]. Moreover, monolith catalyst has lower pressure drop and better mass transfer performance than the traditional pellet catalyst. In this work the palladium-based monolith catalyst using SiO_2 as the secondary carrier (i.e., $Pd/SiO_2/COR$ monolith catalyst) was proposed for the catalytic hydrogenation of eAQ for the synthesis of H_2O_2, aiming to combine the advantages of palladium active centers (high activity) and monolith honeycomb support (low pressure drop and high capacity). Then, the prepared

* Corresponding authors.
E-mail addresses: leizhg@mail.buct.edu.cn (Z. Lei), fangxiangchen.fshy@sinopec.com (X. Fang).

http://dx.doi.org/10.1016/j.cattod.2016.03.023
0920-5861/

Pd/SiO_2/COR monolith catalysts were characterized by XRD, SEM, BET, H_2-TPR, ICP-AES, and XPS. Finally, the influence of different operating parameters (catalyst content, reaction temperature, pressure, flow rates of inlet H_2 and eAQ solution, and concentration of eAQ solution) on reaction performance was investigated to get the optimum condition for the synthesis of H_2O_2 over Pd/SiO_2/COR catalyst.

2. Experimental

2.1. Preparation of Pd/SiO_2/COR

A series of Pd/SiO_2/COR monolith catalysts were prepared using coating method according to the following four steps. 1) The pretreatment of cordierite monolithic support: the cordierite monolith samples with a diameter of 20 mm and a height of 10 mm were cut from a commercial honeycomb cordierite (φ 101.6 × 127 mm, 400 cpi square channels), and then pretreated using 15 wt% nitric acid solution at 80 °C for 4 h. Afterwards, the pretreated cordierite monolith samples were washed using deionized water to neutral, dried at 100 °C for 4 h and calcined in a Muffle furnace at 550 °C for 4 h; 2) The coating of SiO_2: the cordierite samples after acid treatment were immersed into the silicon sol solution for 5 min and then dried at 100 °C. The coating procedure was repeated several times. Then the samples (SiO_2/COR) were dried at 100 °C for 4 h and calcined at 550 °C for 4 h; 3) The coating of active catalyst Pd: the samples obtained in step 2) were immersed into the 6 mg·mL^{-1} $PdCl_2$ aqueous solution, and then dried as the coating of SiO_2. The procedure was repeated several times to achieve the desired coating amount of Pd. Thus, a series of $PdCl_2/SiO_2$/COR precursors can be obtained; 4) The activation of precursor: the precursor was calcined at 550 °C to remove the chlorine element, and the Pd/SiO_2/COR monolith catalysts were obtained. The theoretical content means that the Pd in the solution is all supported onto the catalyst based on theoretical calculation for loading target content.

2.2. Characterization

X-ray diffraction (XRD) patterns were collected from a Bruker D8 Advance X-ray diffractometer (40 kV, 40 mA) using Cu-Kα radiation (λ = 0.15418 nm). Data were recorded in the 2θ range from 5° to 50° with a step size of 5° and a count time of 1 min per step.

Scanning electron microscopy (SEM) micrographs were recorded on a JEOL JSM-6701F microscope working at 5.0 kV accelerating voltage. Before observation, the samples were subsequently sputter coated with a thin gold film by an ion-sputtering instrument to make the sample conductive.

The Brunauer-Emmett-Teller (BET) specific surface areas of the catalysts were determined by using a Micromeritics ASAP-2020 sorptometer apparatus. Before the measurement of BET, the samples were degassed at 350 °C for at least 5 h under vacuum. The total surface area was calculated according to the BET method.

Hydrogen temperature programmed reduction (H_2-TPR) experiments of the calcined Pd/SiO_2/COR catalysts were carried out on a Thermo Electron TPD/R/O 1100 series instrument equipped with a thermal conductivity detector (TCD). The samples were reduced in a stream of 10% H_2 flow (volume fraction, balanced by Ar) with the flowrate of 30 mL min^{-1} and heating rate of 10 K min^{-1} from 273 to 1173 K.

Inductively coupled plasma-atomic emission spectrometry (ICP-AES) experiments of the calcined Pd/SiO_2/COR catalysts were performed on a Shimadzu Corporation-ICP-7500.

X-ray photoelectron spectroscopy (XPS) spectra were performed on an ESCALAB 250 photoelectron spectrometer (Thermo Fisher Scientific, USA). XPS spectra were recorded using monochromated Al Kα excitation at pass energies of 200 eV for survey and 30 eV for high-resolution scans. The binding energy calibration of all spectra was referenced to the adventitious carbon (C1s) signal at 284.6 eV to reduce the charging effect of samples.

2.3. Catalytic activity measurement Pd/SiO_2/COR

The catalytic hydrogenation of eAQ was performed in a stainless steel fixed-bed reactor (20 mm in inner diameter and 450 mm in length) with a central thermocouple to measure the temperature of reaction zone under atmospheric pressure. There are 11 elements of Pd/SiO_2/COR monolith catalysts packed in the constant temperature zone of the reactor and embedded between the pretreated cordierite supports in both sides of the reaction zone to support the catalyst bed. The 11 elements were tightly installed so that the gaps between each other, as well as between monolith section and stainless steel tube, can be ignored. Before the hydrogenation experiments, the catalysts were reduced in situ under hydrogen atmosphere at 150 °C, and then the reactor was cooled down to the reaction temperature. The feedstock (eAQ dissolved in C9 aromatics and trioctyl phosphate mixture with a volume ratio of 3:1, the concentration of eAQ solution was 60 g L^{-1}) was then pumped into the reactor by double-plunger pump, while hydrogen was input through a gas mass flow meter. Then, the hydrogenated anthraquinone working solution was pumped into the oxidation device for oxidation reaction by the air from oil-free air generator (GC-ready SPB-5000 Automatic Air Source) to produce H_2O_2 at room temperature. Afterwards, the oxidated working solution (H_2O_2 solution) was extracted with 25.2 wt% sulfuric acid solution several times.

The content of H_2O_2 obtained from the oxidation of $eAQH_2$ was measured by the $KMnO_4$ titration. The yield of H_2O_2 $\left((H_2O_2(mol)/EAQ(mol)) \cdot 100\%\right)$ and the space time yield (STY, $(H_2O_2(g)/Pd(g))/time(h)$) were introduced to characterize the catalytic performance of Pd/SiO_2/COR catalysts with different Pd contents.

3. Results and discussion

3.1. Characterization of monolith catalysts

3.1.1. XRD analysis

Fig. 1 shows the XRD patterns of the cordierite (COR), the pretreated COR, the SiO_2/COR, and the Pd/SiO_2/COR monolith catalysts

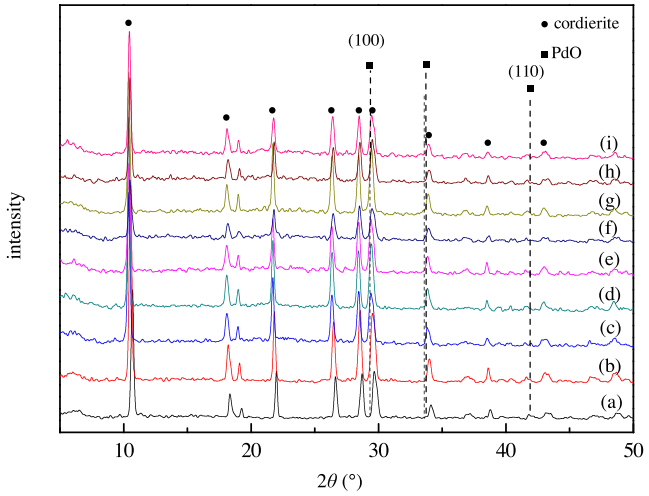

Fig. 1. XRD patterns of Pd/SiO_2/COR samples with various contents of Pd. (a) COR; (b) pretreated COR; (c) SiO_2/COR; (d) 0.6% Pd/SiO_2/COR; (e) 1.0% Pd/SiO_2/COR; (f) 1.2% Pd/SiO_2/COR; (g) 1.5% Pd/SiO_2/COR; (h) 1.7% Pd/SiO_2/COR; (i) 2.2% Pd/SiO_2/COR.

Please cite this article in press as: Y. Guo, et al., Synthesis of hydrogen peroxide over Pd/SiO_2/COR monolith catalysts by anthraquinone method, Catal. Today (2016), http://dx.doi.org/10.1016/j.cattod.2016.03.023

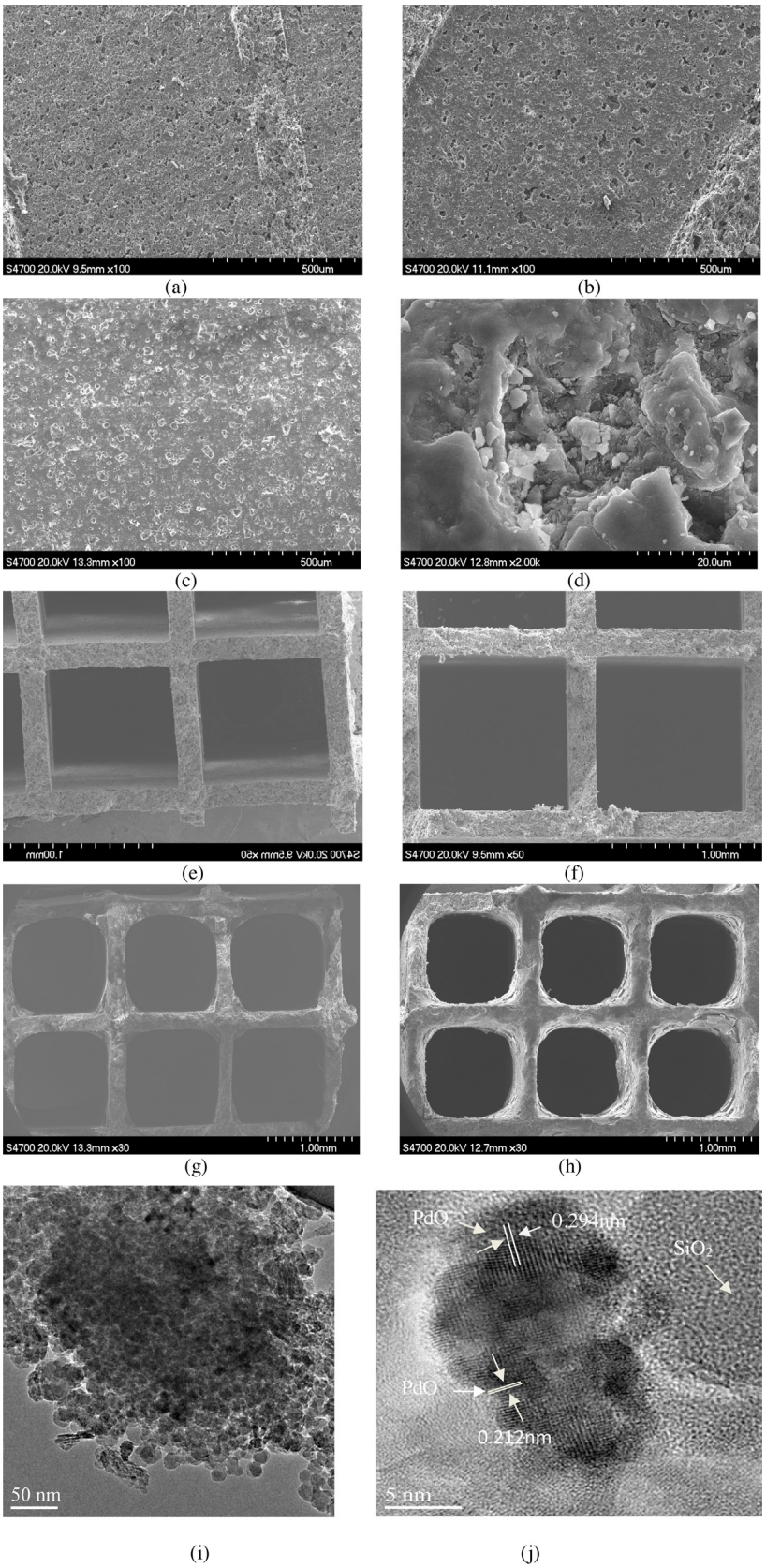

Fig. 2. SEM micrographs. (a) wall surface of COR; (b) wall surface of the pretreated COR; (c) wall surface of SiO_2/COR; (d) wall surface of Pd/SiO_2/COR; (e) cross section of COR; (f) cross section of the pretreated COR; (g) cross section of SiO_2/COR; (h) cross section of Pd/SiO_2/COR. (i) and (j) HRTEM images of 1.5%Pd/SiO_2/COR catalyst.

Please cite this article in press as: Y. Guo, et al., Synthesis of hydrogen peroxide over Pd/SiO_2/COR monolith catalysts by anthraquinone method, Catal. Today (2016), http://dx.doi.org/10.1016/j.cattod.2016.03.023

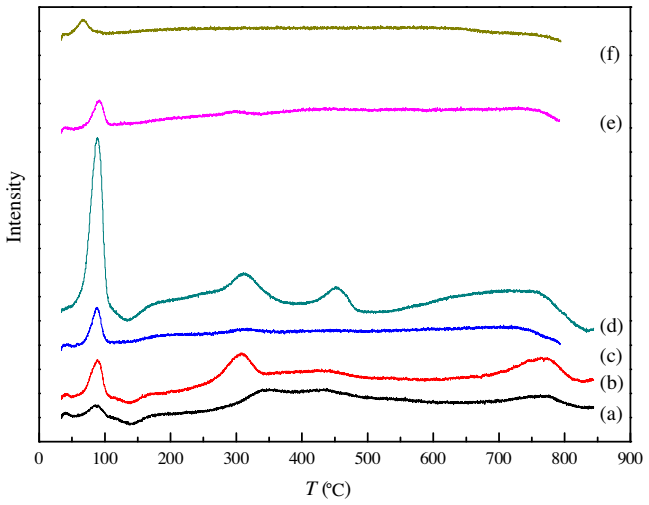

Fig. 3. H_2-TPR spectra of Pd/SiO_2/COR samples with various contents of Pd. (a) 0.6% Pd/SiO_2/COR; (b) 1.0% Pd/SiO_2/COR; (c) 1.2% Pd/SiO_2/COR; (d) 1.5% Pd/SiO_2/COR; (e) 1.7% Pd/SiO_2/COR; (f) 2.2% Pd/SiO_2/COR.

with different Pd contents. It can be seen that the diffraction peaks are typical peaks of cordierite, which are consistent with the XRD standard PDF card no. 089-1487 [35]. PdO peak is overlapped with cordierite peak at $2\theta = 33.6^\circ$, 33.9°, 29.3° and other peak of PdO peak is at $2\theta = 41.9^\circ$, which are consistent with the XRD standard PDF card no.06-0515. After treatment, the cordierite peaks did not decrease and were kept constant. In addition, the intensity of the cordierite peaks after treatment is the same as before treatment, indicating that the acid treatment and calcination did not change the cordierite structure.

3.1.2. SEM and BET analysis

Fig. 2 illustrates the SEM micrographs on the surface and cross section of the COR, SiO_2/COR, and Pd/SiO_2/COR monolith catalysts. The macropores on the cordierite surface become bigger after acid treatment. The cross sectional view of the SiO_2/COR sample shows that the colloidal silica washcoat tends to accumulate in the corners of monolith structure. Fig. 2(c) shows that SiO_2 has a uniform distribution on the surface of COR channel wall, to provide more surface area to coat the catalytic center Pd. However, no information has been obtained about palladium, which is probably due to the relative low Pd content and the good dispersion of Pd. Thus, the small Pd particles were not detected by SEM. From the HRTEM image as shown in Fig. 2(i), it can be seen that PdO dispersed uniformly and the interplanar spacing (0.294 nm and 0.212 nm) corresponded to the (100) and (110) planes of PdO, while SiO_2 is amorphous.

The total surface area was calculated according to the BET method. The results show that after the acid treatment of COR, the BET surface area increases from less than 1.0–13.5 $m^2\,g^{-1}$. After the coating of SiO_2 the BET surface area achieves to 55.3 $m^2\,g^{-1}$, while the coating of catalytic component Pd can further increase the surface area (e.g., 60.8 $m^2\,g^{-1}$ for 1.5% Pd/SiO_2/COR) but not so obviously, which are consistent with the SEM results.

3.1.3. H_2-TPR analysis

TPR results of Pd/SiO_2/COR catalysts demonstrate that in each case four reduction peaks can be observed in the reduction region (see Fig. 3). The low-temperature reduction peak at 90 °C is assigned to the reduction of PdO species on the surface of the catalysts, which makes the most contribution to catalytic hydrogenation of eAQ. The high-temperature peaks at 300, 450 and 750 °C are assigned to the reduction of PdO in the inner layer and other surface oxygen. It can be seen that Pd/SiO_2/COR catalyst with the content of 1.5% (which is the theoretical content of Pd) has the strongest peak at 90 °C when compared to others, and also has stronger high-temperature peaks than others. The results indicated that 1.5% Pd/SiO_2/COR catalyst has the most PdO content on the surface of monolith channel. That is to say, more immersion times of SiO_2/COR into $PdCl_2$ solution would no longer be benefit to the catalytic hydrogenation of eAQ. It is reported that Pd plays a key role in hydrogenation stage of anthraquinone hydrogenation reaction [36,37]. Thus, before the hydrogenation experiments, the Pd/SiO_2/COR catalysts in PdO state must be reduced in situ under hydrogen atmosphere at 150 °C to obtain the Pd state catalyst.

Table 1
ICP-AES results of Pd actual content on different Pd/SiO_2/COR catalysts.

Sample	Theoretical content of Pd	Actual content of Pd
0.6% Pd/SiO_2/COR	0.6%	0.04%
1.0% Pd/SiO_2/COR	1.0%	0.07%
1.2% Pd/SiO_2/COR	1.2%	0.08%
1.5% Pd/SiO_2/COR	1.5%	0.10%
1.7% Pd/SiO_2/COR	1.7%	0.30%
2.2% Pd/SiO_2/COR	2.2%	0.40%

Table 2
XPS Results of Pd $3d_{5/2}$ for different Pd/SiO_2/COR catalysts.

Sample	Pd $3d_{5/2}$ binding energy (ev)	Element composition (%)		
		Si_{2p}	O_{1s}	Pd_{3d}
0.6% Pd/SiO_2/COR	337.10	32.63	56.05	0.13
1.0% Pd/SiO_2/COR	335.60	30.24	61.22	0.16
1.2% Pd/SiO_2/COR	335.90	31.49	62.70	0.16
1.5% Pd/SiO_2/COR	335.75	28.59	61.14	0.84
1.7% Pd/SiO_2/COR	336.45	31.09	61.48	0.44
2.2% Pd/SiO_2/COR	336.80	34.33	61.20	0.10

3.1.4. ICP analysis

ICP-AES experiments were carried out to measure the actual element contents in the bulk coating of Pd/SiO_2/COR catalysts, and the results are listed in Table 1. There is a large difference between the theoretical and actual (ICP-AES result) contents of Pd for all tested samples, indicating that the interaction between SiO_2 coating and Pd species is not strong enough to coat more active component Pd. However, the theoretical content of Pd and ICP-AES results exhibit the similar trend.

3.1.5. XPS analysis

The XPS technology was used to study the chemical state of Pd species and relative contents of different elements on the Pd/SiO_2/COR catalyst channel surface. The XPS spectra of tested samples are illustrated in Fig. 4, where the normalized intensity data were adopted. It can be seen that Pd species is mainly in the state of PdO, no $PdCl_2$ being detected, indicating that chlorine element was completely removed during the calcination process. In this work, Pd $3d_{5/2}$ region was observed at binding energies in the range of 335.6–337.1 eV. The binding energy of Pd $3d_{5/2}$ is consistent with that as reported in Ref. [38].

The detailed element compositions of Pd/SiO_2/COR catalysts are listed in Table 2. With the increase of theoretical content of Pd, the actual Pd element on the monolith channel surface first increases and then decreases. This means that 1.5% Pd/SiO_2/COR catalyst is the optimum, which is consistent with the result of H_2-TPR as mentioned above.

3.2. Catalytic activity

The influence of different operating parameters (catalyst content, reaction temperature, reaction pressure, flow rates of inlet

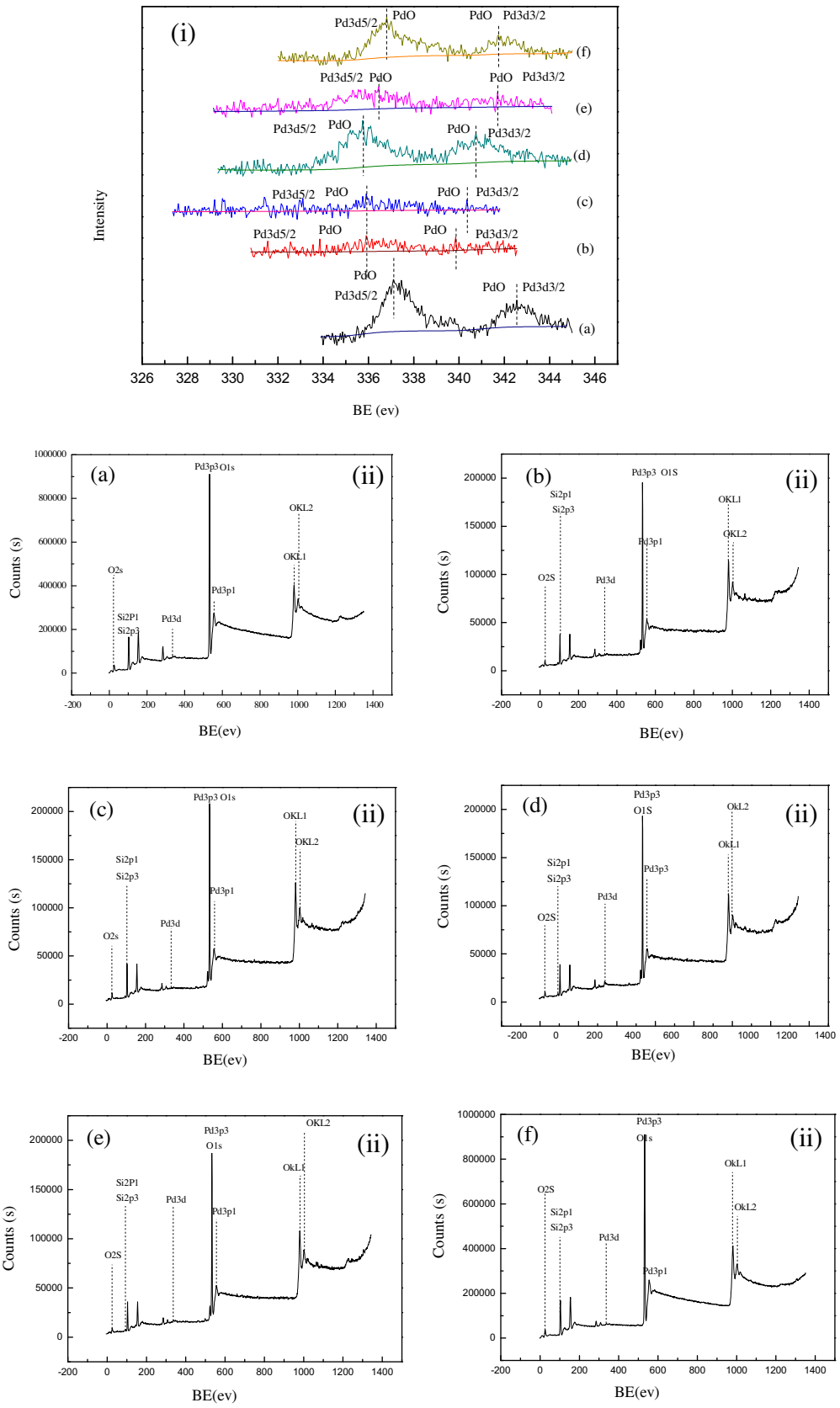

Fig. 4. XPS Pd3d spectra (i) and the survey (ii) of samples. (a) 0.6% Pd/SiO_2/COR; (b) 1.0% Pd/SiO_2/COR; (c) 1.2% Pd/SiO_2/COR; (d) 1.5% Pd/SiO_2/COR; (e) 1.7% Pd/SiO_2/COR; (f) 2.2% Pd/SiO_2/COR.

Please cite this article in press as: Y. Guo, et al., Synthesis of hydrogen peroxide over Pd/SiO_2/COR monolith catalysts by anthraquinone method, Catal. Today (2016), http://dx.doi.org/10.1016/j.cattod.2016.03.023

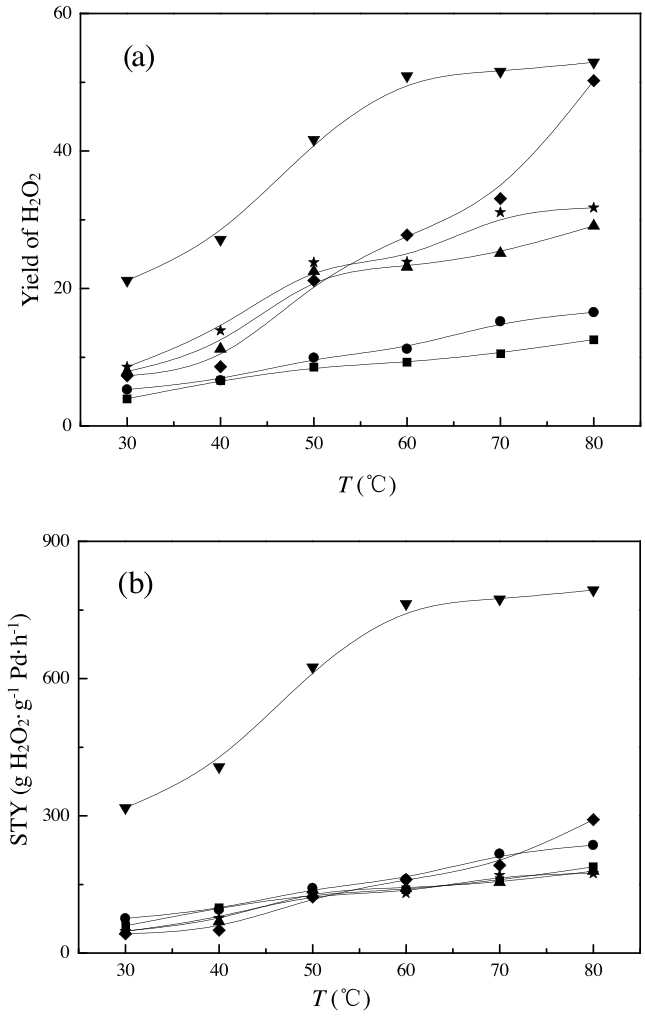

Fig. 5. Influence of reaction temperature on the yield of H_2O_2 and the STY. (Reaction conditions: atmospheric pressure, concentration of eAQ solution = 60 g L^{-1}, flow rate of eAQ solution = 0.7 mL min^{-1}, flow rate of H_2 = 100 mL min^{-1}).
■, 0.6% Pd/SiO_2/COR; ●, 1.0% Pd/SiO_2/COR; ▲, 1.2% Pd/SiO_2/COR; ▼, 1.5% Pd/SiO_2/COR; ♦, 1.7% Pd/SiO_2/COR; ★, 2.2% Pd/SiO_2/COR.

H_2 and eAQ solution, and concentration of eAQ solution) on reaction performance (i.e., the yield of H_2O_2 and the space time yield (STY)) was investigated for the synthesis of H_2O_2 over Pd/SiO_2/COR catalyst.

The influence of reaction temperature from 30 to 80 °C using Pd/SiO_2/COR catalysts with different Pd contents is illustrated in Fig. 5. The result shows that temperature has an important influence on reaction performance as reported by Halder and Lawal [22]. With the increase of reaction temperature, both the yield of H_2O_2 and the STY increase gradually, the optimum temperature being 80 °C. Moreover, with the increase of Pd content in Pd/SiO_2/COR catalyst, the yield of H_2O_2 and the STY first increase and then decrease. The Pd/SiO_2/COR catalyst with theoretical Pd content of 1.5% exhibits the highest yield and STY, which is attributed to the 1.5% Pd/SiO_2/COR catalyst having the most actual Pd content on the catalyst channel surface as proved by XPS results. In this case, the yield of H_2O_2 and STY at 80 °C are 53% and 793.2 g H_2O_2 g^{-1} Pd h^{-1}, respectively.

The influence of H_2 pressure is illustrated in Fig. 6(a). It is seen that the increase of both the yield of H_2O_2 and STY is not so obvious in the range of atmospheric pressure to 1.0 MPa, indicating that the catalytic hydrogenation of eAQ is not highly dependent on the H_2 pressure. Fig. 6(b) shows the plot of log(STY) versus log(P_{H2}). It appears that the dependency of rate on hydrogen concentration is almost zero order. Damkohler number (Da) (defined as Da = chemicalreaction rate/external diffusion rate) was introduced to determine whether the hydrogenation process is controlled by chemical reaction or by external diffusion [39]. The external diffusion rate was calculated by the correlation [40], and the chemical reaction rate came from literature [41,42]. The results shows that $Da \geq 10$ (Da = 12–20 when the pressure is in the range of 0.1–1.0 MPa), indicating that the hydrogenation process rate is more predominated by external diffusion than by reaction rate.

When the pressure increase, the saturation concentration of hydrogenation in the working solution should increase which in turn should lead to an increase in the liquid-solid mass transfer rate at the same velocity. Nevertheless, with the increase of the hydrogen pressure at the same mass flow rate, the actual volumetric flow rate of the gas is reduced. Even if the mass transfer rate of hydrogen has effect on the reaction rate, the increase in higher hydrogen mass transfer rate from liquid to catalyst due to higher concentration in the liquid could be offset by the decrease in mass transfer rate due to decrease in velocity, resulting in the reaction rate to be relatively independent of hydrogen pressure. Thus, for the sake of convenience and safety, atmospheric pressure was chosen in the subsequent experiments [22].

The influence of flow rate of feedstock is shown in Figs. 7 and 8. As the inlet H_2 gas flow rate increases, the increase of the yield of H_2O_2 is not clear, while the STY sharply increases. As mentioned above, external diffusion is the controlling step during the hydro-

Please cite this article in press as: Y. Guo, et al., Synthesis of hydrogen peroxide over Pd/SiO_2/COR monolith catalysts by anthraquinone method, Catal. Today (2016), http://dx.doi.org/10.1016/j.cattod.2016.03.023

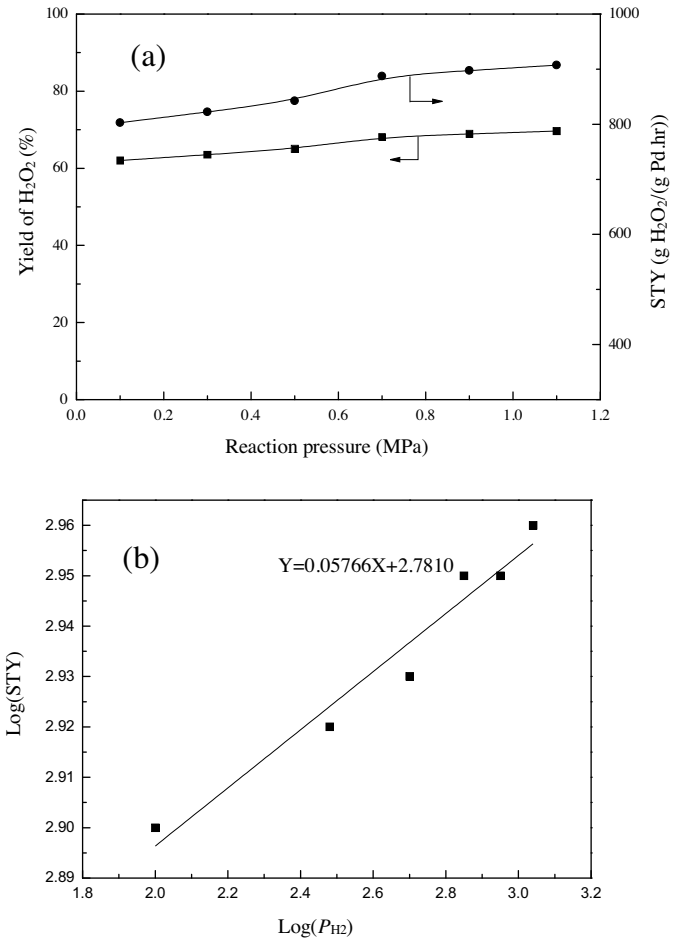

Fig. 6. Influence of H_2 pressure on the yield of H_2O_2 and the STY (a) and the plot of log(STY) vs. log(P_{H2}) (b) (reaction conditions: temperature = 80 °C, concentration of eAQ solution = 60 g L^{-1}, flow rate of eAQ solution = 0.7 mL min^{-1}, flow rate of H_2 = 100 mL min^{-1}, 1.5% Pd/SiO_2/COR catalyst).

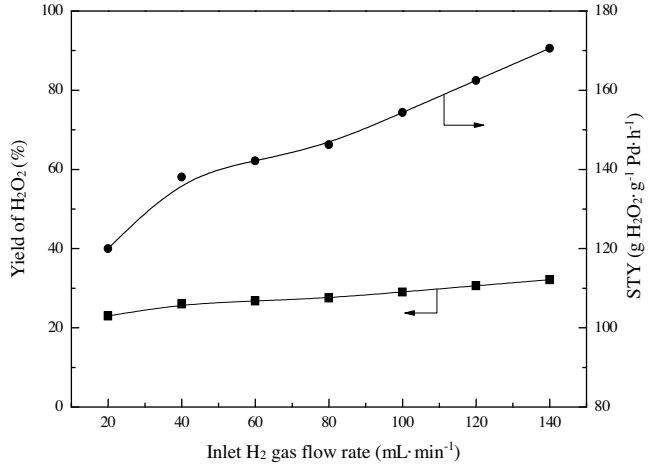

Fig. 7. Influence of inlet H_2 gas flow rate on the yield of H_2O_2 and the STY. (Reaction conditions: atmospheric pressure, temperature = 80 °C, concentration of eAQ solution = 60 g L^{-1}, flow rate of eAQ solution = 0.7 mL min^{-1}, 1.2% Pd/SiO_2/COR catalyst).

genation process because $Da \geq 10$ when the gas and liquid flow rates are in the range of 20–140 mL min^{-1} and 0.3–1.3 mL min^{-1}, respectively. As the flow rate of H_2 increases, the gas has better dispersion into the eAQ solution, leading to a higher mass transfer rate. Furthermore, with more H_2 gas, the reactants H_2 and eAQ on the active Pd sites will contact sufficiently. Considering the balance between the yield of H_2O_2 and the STY, the H_2 flow rate at 100 mL min^{-1} would be more appropriate. From Fig. 8, it can be seen that both the yield of H_2O_2 and the STY increase with the increase of eAQ solution flow rate. The higher the liquid flow rate, the higher the mass transfer rate. When the eAQ solution flow rate is above 0.7 mL min^{-1}, the STY increases slowly, indicating that the liquid flow rate 0.7 mL min^{-1} is more appropriate.

From Fig. 9(a), it can be seen that the increase in the eAQ concentration brings about the increase in the yield of H_2O_2 and the STY. The higher the eAQ concentration, the higher the yield of H_2O_2. However, when the concentration is higher than 60 g L^{-1}, the increase becomes slower than before due to the limiting active Pd sites. If the active sites are not saturated, the yield of H_2O_2 increases significantly with the increase of eAQ concentration. However, if the Pd active sites are saturated, the yield of H_2O_2 almost does not change. As a result, the eAQ concentration 60 g L^{-1} is chosen for the eAQ catalytic hydrogenation. Fig. 9(b) shows the plot of log(STY) versus log(C_{eAQ}), and the slop (0.95) means that the reaction rate has appropriately a first-order dependence on the eAQ concentration, which is consistent with the conclusion by Halder and Lawal [22] and Santacesaria et al. [43] that the reaction rate has a first-order dependency on the EAQ concentration in both microreactor and conventional reactors.

Furthermore, stability test was done for the hydrogenation reaction of eAQ. Fig. 10 shows that the yield of H_2O_2 keeps around 52% during 48 h.

Please cite this article in press as: Y. Guo, et al., Synthesis of hydrogen peroxide over Pd/SiO_2/COR monolith catalysts by anthraquinone method, Catal. Today (2016), http://dx.doi.org/10.1016/j.cattod.2016.03.023

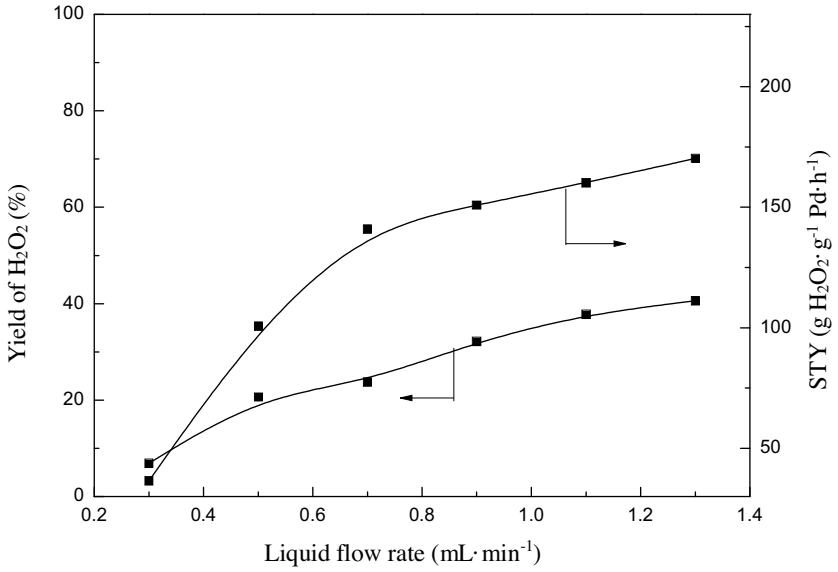

Fig. 8. Influence of eAQ solution flow rate on the yield of H_2O_2 and the STY. (Reaction conditions: atmospheric pressure, temperature = 80 °C, concentration of eAQ solution = 60 g L^{-1}, flow rate of H_2 = 100 mL min^{-1}, 1.2% Pd/SiO_2/COR catalyst).

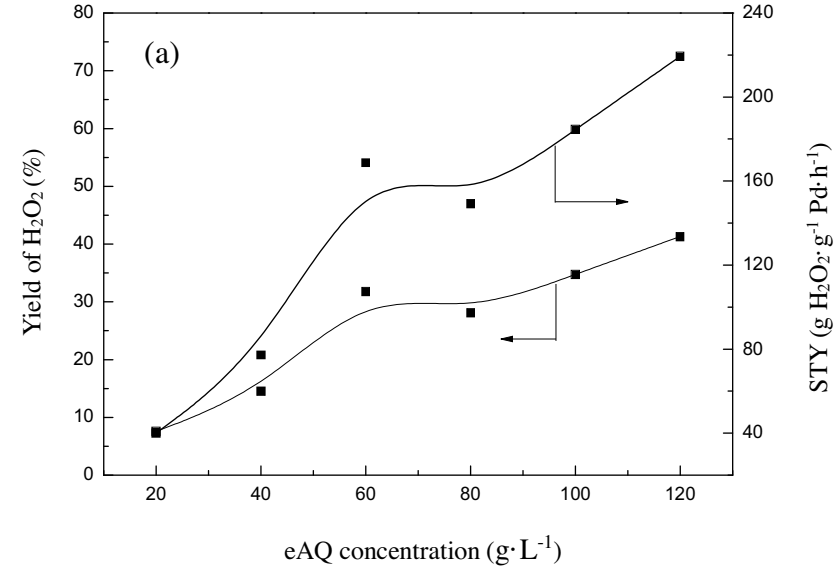

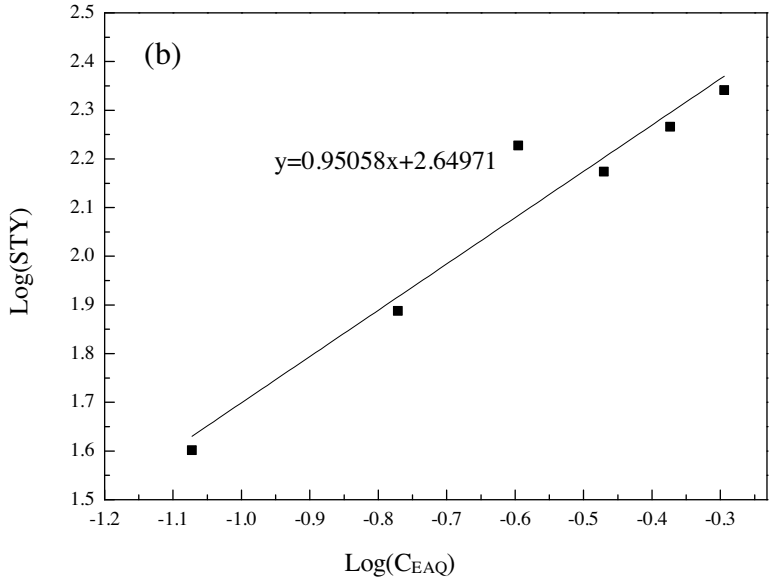

Fig. 9. Influence of eAQ concentration on the yield of H_2O_2 and the STY (a) and the plot of log(STY) vs. log(C_{EAQ}) (b). (Reaction conditions: atmospheric pressure, temperature = 80 °C, flow rate of eAQ solution = 0.7 mL min^{-1}, flow rate of H_2 = 100 mL min^{-1}, 1.2% Pd/SiO_2/COR catalyst).

Please cite this article in press as: Y. Guo, et al., Synthesis of hydrogen peroxide over Pd/SiO_2/COR monolith catalysts by anthraquinone method, Catal. Today (2016), http://dx.doi.org/10.1016/j.cattod.2016.03.023

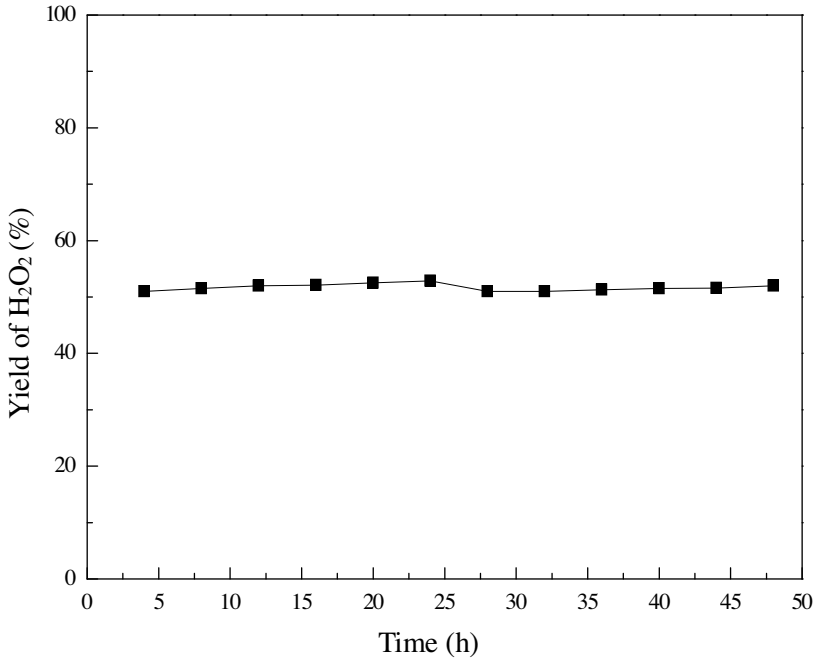

Fig. 10. Stability test for Pd/SiO_2/COR catalyst. (Reaction conditions: atmospheric pressure, temperature = 80 °C, concentration of eAQ solution = 120 g L^{-1}, flow rate of eAQ solution = 0.7 mL min^{-1}, flow rate of H_2 = 100 mL min^{-1}, 1.5% Pd/SiO_2/COR catalyst).

4. Conclusions

In this work, a series of Pd/SiO_2/COR catalysts were successfully prepared by impregnation method and were characterized by XRD, SEM, HRTEM, BET, H_2-TPR, ICP-AES, and XPS. The results showed that Pd element is mainly in the state of PdO in the presence of lattice fringes on the catalyst surface, and 1.5% Pd/SiO_2/COR catalyst with theoretical Pd content of 1.5% has the most PdO content on the surface of monolith channel. On this basis, the influence of different operating parameters on reaction performance was investigated for the synthesis of H_2O_2 over Pd/SiO_2/COR catalyst. It was found that the STY can achieve 793.2 g H_2O_2 g^{-1} Pd h^{-1} over the optimum catalyst 1.5% Pd/SiO_2/COR monolith catalyst on the appropriate conditions for the synthesis of H_2O_2: temperature 80 °C, atmospheric pressure, the inlet H_2 and eAQ flow rates of 100 and 0.7 mL min^{-1}, respectively, eAQ concentration 60 g L^{-1}. Thus, the monolith catalyst presented in this work is a promising alternative to pellet catalysts for the catalytic hydrogenation of eAQ for the synthesis of H_2O_2.

Acknowledgments

This work was financially supported by the National Natural Science Foundation of China under Grants (Nos. 21476009, 21406007, and U1462104), and State Key Laboratory of Heavy Oil Processing (SKLHOP201502).

References

[1] H. Shang, H. Zhou, Z. Zhu, W. Zhang, J. Ind. Eng. Chem. 18 (2012) 1851–1857.
[2] Hydrogen Peroxide, Wikipedia, The Free Encyclopedia, Available from, 2006 http://en.wikipedia.org.
[3] H. Chen, D. Huang, X. Su, J. Huang, X. Jing, M. Du, D. Sun, L. Jia, Q. Li, Chem. Eng. J. 262 (2015) 356–363.
[4] R. Aksela, J. Paloniemi. Hydrogenation of a working solution in a hydrogen peroxide production process, US 6749727, (2004).
[5] G. Goor, E. Staab, J. Glenneberg. Process for the preparation of hydrogen peroxide by the anthraquinone cyclic process, US 7238335, (2007).
[6] J. Petr, L. Kurc, Z. Bělohlav, L. Cerveny, Chem. Eng. Process. 43 (2004) 887–894.
[7] A. Drelinkiewicz, A. Waksmundzka-Góra, J. Mol. Catal. A: Chem. 258 (2006) 1–9.
[8] R. Hong, J. Feng, Y. He, D. Li, Chem. Eng. Sci. 135 (2015) 274–284.
[9] A. Drelinkiewicz, A. Waksmundzka-Góra, J. Mol. Catal. A: Chem. 246 (2006) 167–175.
[10] A. Drelinkiewicz, A. Waksmundzka-Góra, J.W. Sobczak, J. Stejskal, Appl. Catal. A: Gen. 333 (2007) 219–228.
[11] R. Kosydar, A. Linkiewicz, J.P. Ganhy, Catal. Lett. 139 (2010) 105–113.
[12] P. Tang, Y. Chai, J. Feng, Y. Feng, Y. Li, D. Li, Appl. Catal. A: Gen. 469 (2014) 312–319.
[13] A. Linkiewicz, J. Mol. Catal. A: Chem. 101 (1995) 61–74.
[14] Z. Guo, J. Feng, Y. Feng, D.G. Evans, D. Li, Appl. Catal. A: Gen. 401 (2011) 163–169.
[15] C. Shen, Y. Wang, J. Xu, Y. Lu, G. Luo, Chem. Eng. J. 173 (2011) 226–232.
[16] R. Kosydar, A. Linkiewicz, E. Lalik, J. Gurgual, Appl. Catal. A: Gen. 402 (2011) 121–131.
[17] A. Drelinkiewicz, M. Hasik, J. Mol. Catal. A: Chem. 177 (2001) 149–164.
[18] Y. Zhu, L. Yu, X. Wang, Y. Zhou, H. Ye, Catal. Commun. 40 (2013) 98–102.
[19] E. Santacesaria, M.D. Serio, R. Velotti, U. leone, Ind. Eng. Chem. Res. 33 (1994) 277–284.
[20] X. Gao, Y. Zhao, S. Wang, Y. Yin, B. Wang, X. Ma, Chem. Eng. Sci. 66 (2001) 3513–3522.
[21] D. Gudarzi, W. Ratchananusorn, I. Turunen, M. Heinonen, T. Salmi, Catal. Today 248 (2015) 69–79.
[22] R. Halder, A. Lawal, Catal. Today 125 (2007) 48–55.
[23] G. Liu, Y. Duan, Y. Wang, L. Wang, Z. Mi, Chem. Eng. Sci. 60 (2005) 6270–6278.
[24] T. Ishihara, R. Nakashima, Y. Ooishi, H. Hagiwara, M. Matsuka, S. Ida, Catal. Today 248 (2015) 35–39.
[25] S. Sterchele, P. Biasi, P. Centomo, P. Canton, S. Campestrini, T. Salmi, M. Zecca, Appl. Catal. A: Gen. 468 (2013) 160–174.
[26] A. Drelinkiewicz, R. Laitinen, R. Kangas, J. Pursiainen, Appl. Catal. A: Gen. 284 (2005) 59–67.
[27] R. Edvinsson, M. Nystrom, M. Silverstrom, A. Sellin, A.C. Dellve, U. Anderson, W. Herrmann, T. Berglin, Catal. Today 69 (2001) 247–252.
[28] F. Kapteijn, T.A. Nijhuis, J.J. Heiszwolf, J.A. Moulijn, Catal. Today 66 (2001) 133–144.
[29] B.P. Barbero, L. Costa-Almeida, O. Sanz, M.R. Morales, L.E. Cadus, M. Montes, Chem. Eng. J. 139 (2008) 430–435.
[30] Z. Lei, C. Wen, J. Zhang, B. Chen, Ind. Eng. Chem. Res. 50 (2011) 5942–5951.
[31] M. Hettel, C. Diehm, B. Torkashvand, O. Deutschmann, Catal. Today 216 (2013) 2–10.
[32] C. Dai, Z. Lei, J. Zhang, Y. Li, B. Chen, Chem. Eng. Sci. 100 (2013) 342–351.
[33] J. Zhang, D. Li, Y. Zhao, Q. Kong, S. Wang, Catal. Commun. 9 (2008) 2565–2569.
[34] X. Li, H. Su, G. Ren, S. Wang, Appl. Catal. A: Gen. (2016), http://dx.doi.org/10.1016/j.apcata.2016.01.011.
[35] Q. Li, P. Wu, L. Lan, H. Liu, S. Ji, Catal. Today 216 (2013) 38–43.
[36] F. Menegazzo, P. Burti, M. Signoretto, M. Manzoli, S. Vankova, F. Boccuzzi, F. Pinna, G. Strukul, J. Catal. 257 (2008) 369–381.
[37] P. Biasi, F. Menegazzo, F. Pinna, K. Eranen, T.O. Salmi, P. Canu, Chem. Eng. J. 176 (2011) 172–177.

Please cite this article in press as: Y. Guo, et al., Synthesis of hydrogen peroxide over Pd/SiO_2/COR monolith catalysts by anthraquinone method, Catal. Today (2016), http://dx.doi.org/10.1016/j.cattod.2016.03.023

[38] I.A. Witońska, M.J. Walock, M. Binczarski, M. Lesiak, A.V. Stanishevsky, S. Karski, J. Mol. Catal. A: Chem. 393 (2014) 248–256.
[39] E. Tronconi, P. Forzatti, AIChE J. 38 (2004) 201–210.
[40] D. Liu, J. Zhang, D. Li, Q. Kong, T. Zhang, S. Wang, AIChE J. 55 (2009) 726–736.
[41] Q. Chen, Inorg. Chem. Ind. 33 (2001) 20–22 (in Chinese).
[42] Z. Zhao, X. Tang, J. Zhou, Dawn Chem. Ind. 2 (1986) 8–14 (in Chinese).
[43] E. Santacesaria, M.D. Serio, A. Russo, U. Leone, R. Velotti, Chem. Eng. Sci. 54 (1999) 2799–2806.

Please cite this article in press as: Y. Guo, et al., Synthesis of hydrogen peroxide over Pd/SiO_2/COR monolith catalysts by anthraquinone method, Catal. Today (2016), http://dx.doi.org/10.1016/j.cattod.2016.03.023